Structural Determinants of HscA Peptide-Binding Specificity†

Timothy L. Tapley,‡ Jill R. Cupp-Vickery, and Larry E. Vickery*

Department of Physiology and Biophysics, University of California, Irvine, California 92697

Received March 28, 2006; Revised Manuscript Received May 5, 2006

ABSTRACT: The Hsp70-class molecular chaperone HscA interacts specifically with a conserved ^{99}LPPVK^{103} motif of the iron−sulfur cluster scaffold protein IscU. We used a cellulose-bound peptide array to perform single-site saturation substitution of peptide residues corresponding to Glu^{98}−Ile^{104} of IscU to determine positional amino acid requirements for recognition by HscA. Two mutant chaperone forms, HscA(F426A) with a DnaK-like arch structure and HscA(M433V) with a DnaK-like substrate-binding pocket, were also studied. Wild-type HscA and HscA(F426A) exhibited a strict preference for proline in the central peptide position (ELPPVKI), whereas HscA(M433V) bound a peptide containing a Pro→Leu substitution at this location (ELPLVKI). Contributions of Phe^{426} and Met^{433} to HscA peptide specificity were further tested in solution using a fluorescence-based peptide-binding assay. Bimane-labeled HscA and HscA(F426A) bound ELPPVKI peptides with higher affinity than leucine-substituted peptides, whereas HscA(M433V) favored binding of ELPLVKI peptides. Fluorescence-binding studies were also carried out with derivatives of the peptide NRLLLTG, a model substrate for DnaK. HscA and HscA(F426A) bound NRLLLTG peptides weakly, whereas HscA(M433V) bound NRLLLTG peptides with higher affinity than IscU-derived peptides ELPPVKI and ELPLVKI. These results suggest that the specificity of HscA for the LPPVK recognition sequence is determined in part by steric obstruction of the hydrophobic binding pocket by Met^{433} and that substitution with the Val^{433} sidechain imparts a broader, more DnaK-like, substrate recognition pattern.

Hsp70-family chaperones are involved in a broad range of protein-folding processes, including folding of newly synthesized proteins, trafficking within the cell, and refolding of stress-denatured proteins (*1*−*7*). Participation in such diverse pathways is dependent upon the ability of different Hsp70 family members to discriminate between numerous potential substrates present in the cell. Hsp70s interact with short unfolded segments of polypeptide chains, and binding is nucleotide-dependent, with the HscA·ADP complex exhibiting higher affinity and slower exchange rates than the HscA·ATP complex (*8*−*12*). Recognition and selection of peptides is determined both by the intrinsic specificity of the Hsp70 substrate-binding domain (SBD)[1] (*13*−*17*) and by J-protein co-chaperones, which act to direct substrates to their Hsp70 partners and to stimulate Hsp70 ATPase activity to stabilize complex formation (*7*, *18*−*23*).

Escherichia coli contains three Hsp70 isoforms, DnaK, HscA, and HscC, with different cellular functions. DnaK is involved in diverse protein-folding processes, including stress responses and interactions with a wide range of polypeptide substrates (*15*), whereas HscA appears to function specifically in iron−sulfur protein biosynthesis and to interact only with the Fe−S scaffold protein IscU (*24*, *25*). The exact cellular role of HscC is not known, but HscC lacks general chaperone activity and may play an as yet undefined role in responses to heavy-metal toxicity and/or UV irradiation damage (*26*). At present, little is known about factors contributing to the differences in specificity of the three Hsp70s. Crystallographic and solution NMR studies of complexes of the SBD of DnaK with the model peptide substrate NRLLLTG revealed that the peptide is bound in an extended conformation in a hydrophobic cleft between the β subdomain and α-helical lid (*27*, *28*). The complex is stabilized by nonpolar interactions involving sidechains of the peptide and by hydrogen-bonding interactions with the peptide backbone. Selectivity appears to be greatest at the central hydrophobic pocket (position "0") of DnaK occupied by Leu4 of the NRLLLTG peptide. Screening of cellulose-bound peptide libraries with DnaK showed a strong preference for nonpolar residues in the peptide core, especially leucine, and enrichment of basic residues in flanking segments; binding of acidic residues was disfavored (*15*).

Studies of the substrate-binding specificity of HscA have revealed a different recognition pattern from that of DnaK. HscA binds selectively to the conserved ^{99}LPPVK^{103} sequence of IscU, and peptide binding and alanine scanning of this region of IscU indicated that the central proline, corresponding to Pro^{101} of IscU, was the most critical residue (*29*). The preference of HscA for proline is in contrast to typical DnaK substrates in which proline binding is disfavored (*15*). In addition, solution fluorescence studies showed that IscU-derived peptides bind HscA in an orientation that is reversed relative to that observed in the DnaK-

† This work was supported by National Institutes of Health Grant GM54264.

* To whom correspondence should be addressed. Telephone: (949) 824-6580. Fax: (949) 824-8540. E-mail: lvickery@uci.edu.

‡ Current address: Department of Molecular, Cellular, and Developmental Biology, University of Michigan, Ann Arbor, MI 48109.

[1] Abbreviations: SBD, substrate-binding domain; rmsd, root-mean-square deviation; HKM buffer, 50 mM HEPES-KOH, 150 mM KCl, and 10 mM $MgCl_2$ at pH 7.5. The abbreviations used for synthetic peptides are given in Table 1.

10.1021/bi0606187 CCC: $33.50
Published on Web 06/07/2006

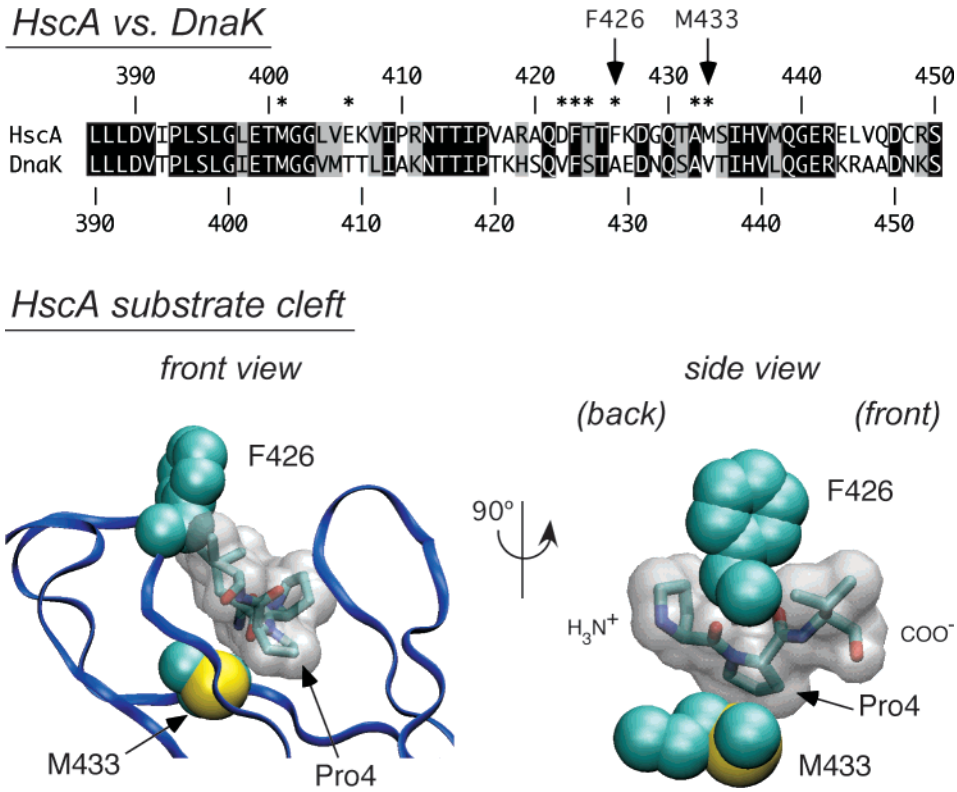

FIGURE 1: Substrate-binding region of HscA. (Upper panel) Sequence alignment of residues 387−450 of *E. coli* HscA with the homologous region of *E. coli* DnaK. Amino acid identities are boxed in black, and similarities are boxed in gray. Sidechains of HscA residues positioned within 4 Å of the bound peptide in the HscA(SBD)-ELPPVKIHC crystal structure (*31*) are indicated with asterisks. (Lower panel) Structural representation of the central region of the peptide cleft in the HscA(SBD)-ELPPVKIHC complex (*31*). The standard front view is that used in refs *27* and *31*. HscA residues Phe^{426} and Met^{433} are shown as space-filling models, and central Pro-Pro-Val residues of the bound peptide are represented with gray transparent surfaces (color coding: carbon, cyan; nitrogen, blue; oxygen, red; sulfur, yellow).

(SBD)-NRLLLTG structure (*30*). The crystal structure of an HscA(SBD)-ELPPVKIHC peptide complex confirmed the reverse-binding orientation for this peptide and revealed that Pro4 of the peptide was located in position 0 of the binding cleft (*31*). HscC has been less extensively studied, but analysis of HscC binding to cellulose−peptide scans of several proteins showed a general similarity to DnaK-binding preference, except that proline was slightly enriched in bound peptides, whereas leucine was not (*26*).

The molecular basis of the peptide-binding differences between DnaK, HscA, and HscC is not well-understood. The general structure of the SBDs of DnaK and HscA are very similar, with main-chain atoms displaying a root-mean-square deviation (rmsd) of <0.8 Å (*31*). In addition, most of the residues forming the peptide-binding cleft are identical or alike in the two proteins (Figure 1). Only two residues in direct contact with the central region of the bound peptide differ between DnaK and HscA. One of these, DnaK Ala^{429}/HscA Phe^{426}, forms an arch over the binding cleft. Substitutions for Ala^{429} of DnaK have been shown to have minor effects on substrate specificity (*16*), but in the HscA(SBD) structure, only the β carbon of Phe^{426} makes contact with the peptide. The other difference, DnaK Val^{436}/HscA Met^{433}, occurs near the base of the central hydrophobic pocket at position 0. The sidechain of DnaK Val^{436} makes extensive van der Waals contacts with the central leucine of the NRLLLTG peptide, and the sidechain of HscA Met^{433} makes extensive contacts with the central proline of the ELPPVKIHC peptide. The size of the central pocket is more restricted in HscA because of the larger size of the methionine sidechain compared to the valine sidechain of DnaK, and resulting steric factors could affect peptide-binding specificity.

In the studies described herein, we have used a cellulose-bound peptide array to investigate the positional amino acid requirements for recognition by HscA and we have used two mutant forms, HscA(F426A) and HscA(M433V), to investigate the role of the peptide cleft arch and central pocket in determining peptide-binding specificity. We have also employed a fluorescent peptide-binding assay to quantitatively assess the effect of these mutations on the peptide-binding affinity and the preference for peptide-binding orientation. The results suggest that the arch structure plays a minor role in the specificity of HscA, whereas the nature of the central binding pocket is a major determinant of the substrate-binding properties.

MATERIALS AND METHODS

Mutagenesis, Protein Expression, Purification, and Labeling. Site-specific mutants of HscA were constructed using the QuikChange technique (Stratagene) with oligonucleotides from Integrated DNA Technologies, and mutations were confirmed by DNA sequencing (Laragen, Inc.). HscA(F426A) and HscA(M433V) were constructed using pTrcHscA (*32*) as a template. HscA(F426A/A455C) and HscA(M433V/A455C) were constructed using pTrcHscA(C315S/C448S/A455C) (*30*) as a template, such that both resulting mutants contained codons for a unique cysteine-labeling site. Expression, purification, and bimane labeling of each HscA

Table 1: Sequences of Peptides and Their Tryptophan Derivatives[a]

parent	N-terminal Trp	C-terminal Trp
ELPPVKI (PP)	W-ELPPVKI (W-PP)	not used in this study
ELPLVKI (PL)	W-ELPLVKI (W-PL)	not used in this study
NRLLLTG (NR)	W-NRLLLTG (W-NR)	NRLLLTG-W (NR-W)

[a] Abbreviations used in the text are shown in parenthesis.

protein was performed as described previously (*30*, *32*, *33*). Each variant exhibited chromatographic behavior and far-UV CD spectra similar to that of wild-type HscA, indicating there were no gross structural changes because of the mutations introduced (data not shown). Basal ATPase activity for HscA(M433V) was elevated (0.56 min^{-1}) compared to that of the wild type (0.10 min^{-1}) and HscA(F426A) mutant (0.11 min^{-1}). However, each of the three proteins exhibited similar stimulated activity in the presence of saturating concentrations of HscB and IscU (49.8, 42.2, and 46.4 min^{-1} for the wild type and F426A and M433V mutants, respectively). These observations establish that each form of HscA retains allosteric communication between the NBD and SBD and suggest that these mutations do not result in any gross changes in protein structure or function.

Synthetic Peptides. The synthetic peptides used for fluorescent-binding studies are summarized in Table 1 and were obtained from the PAN facility at Stanford University. Peptides were >95% pure as judged by HPLC and mass spectrometric analysis. Peptide concentrations were determined spectrophotometrically and gravimetrically as previously described (*30*).

Peptide Array Binding Experiments. A custom cellulose-bound peptide library was obtained from Jerini Bio Tools GmbH (Berlin, Germany). Each spot of the array contains a derivative of the dodecapeptide EELELPPVKIHS corresponding to residues 95−106 of IscU(C106S) attached to a cellulose membrane via a C-terminal β-$(Ala)_2$ spacer. Residues of the central ELPPVKI sequence were individually replaced with each of the 20 coded amino acids, except cysteine. The array was probed with 50 nM HscA, HscA(F426A), or HscA(M433V) in 50 mM HEPES-KOH, 150 mM KCl, and 10 mM $MgCl_2$ at pH 7.5 (HKM buffer) containing 1 mM ADP, and bound HscA was transferred to a polyvinylidene fluoride (PVDF) membrane and detected by immunoblotting as described previously (*17*).

Fluorescence Measurements. Fluorescence emission spectra of HscA(A455C)-bimane, HscA(F426A/A455C)-bimane, and HscA(M433V/A455C)-bimane were recorded with a Cary Eclipse Spectrofluorometer (Varian, Inc.). All measurements were performed at 25 °C in HKM buffer using a 4 × 10 mm quartz cuvette as described previously (*30*). Emission spectra (420−520 nm, 10 nm band-pass) of 1 μM bimane-labeled HscA were collected using an excitation wavelength of 390 nm (5 nm band-pass) and a scan rate of 1 nm/s. Peptide titrations were carried out by stepwise additions (5−190 μL) from 1 or 3 mM peptide stocks, and repetitive scans were performed to ensure that equilibrium was reached following each peptide addition. Emission spectra were integrated by taking the sum of emission intensities from 420 to 520 nm. Fluorescence quenching experiments were carried out 2−3 times with similar results, and results from single experiments are shown in Figures 3−5 and Figures S1 and S2 in the Supporting Information.

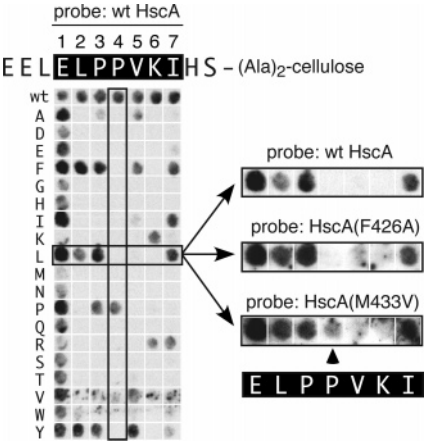

FIGURE 2: Binding of HscA to peptides having amino acid substitutions in the ELPPVKI recognition region. Peptides were displayed in an array and attached via the C terminus to a cellulose membrane using an $(Ala)_2$ spacer. Residues within the ELPPVKI sequence (boxed in black) were individually replaced with the amino acid shown in the left column; spots in the top row contain peptides with the parent (wild-type) sequence. The array was initially probed with wild-type HscA, and binding was detected by immunoblotting. After washing, the array was also probed with HscA(F426A) or HscA(M433V). An expanded view of the leucine substitution row of the array is shown on the right. HscA(M433V) was detected binding a Pro → Leu substituted peptide (ELPLVKI, indicated by the arrow), whereas wild-type HscA and HscA(F426A) exhibit no detectable binding to this peptide. (Some nonspecific binding of the antiserum was evidenced as small, localized spots on the array.)

Structural Modeling. The peptide NRLLLTG was positioned into the HscA peptide-binding cleft by superpositioning of the β subdomains of the DnaK(SBD)-NRLLLTG and HscA(SBD)-ELPPCKIHC structures (DnaK residues 393−503 and HscA residues 390−500; PDB coordinate files 1DKZ and 1U00, respectively). To generate the HscA(M433V) structure, Met^{433} was modeled as valine using FRODO (*34*) and the position of the sidechain was adjusted to match the DnaK structure. The HscA and DnaK structures are nearly identical in the region near the peptide-binding site, and no rearrangement of the HscA backbone was required to accommodate the valine sidechain. Structural representations were generated using VMD (*35*).

Other Methods. Fluorescence emission spectra correction and integration were performed using Excel (Microsoft), and curve fitting was performed using Kaleidagraph (Synergy Software). Peptide concentrations plotted are total concentrations, and therefore, the affinities reported correspond to apparent K_d values.

RESULTS

Sequence Determinants for IscU Peptide Binding to HscA. To investigate the positional amino acid requirements for HscA binding IscU-derived peptides, we utilized a cellulose-bound peptide array to perform the equivalent of site-saturation mutagenesis on the recognition motif. In the array shown in Figure 2, residues of the ELPPVKI sequence were individually replaced with each of the 20 coded amino acids, except cysteine. This generated a 7 × 19 array in which 7 of the 133 peptides are the same as the wild-type sequence and 127 peptides contain single amino acid replacements. A total of 7 wild-type sequence spots were included in the top row as additional controls.

The array was initially probed using wild-type HscA to investigate positional recognition preferences of the natural protein. Significant binding was detected to approximately 37 spots, of which 7 contained the parent ELPPVKI sequence. The majority of the 30 acceptable substitutions correspond to replacement with nonpolar residues (especially phenhylalanine, leucine, and tyrosine), a finding consistent with the general hydrophobic nature of the binding cleft. Residue 1 of the varied region, corresponding to Glu^{98} of IscU, does not appear critical for binding because many substitutions at this location do not impair binding (although lysine, methionine, and arginine appear to be less well-tolerated). The sidechain of the equivalent Glu1 residue in the Hsc(SBD)-ELPPVKIHC crystal structure was observed to interact with Arg^{457} of HscA (*31*). However, alanine-scanning mutagenesis studies of IscU did not show Glu^{98} to be important (*29*), and this finding and the peptide array results suggest that glutamate at this position is not critical for binding. While not essential for high binding affinity, Arg^{457} may serve to disfavor the binding of peptides containing basic residues at this position. Recognition within the core of the recognition sequence (LPPVK) appears to be more stringent, with only a subset of amino acids yielding strong binding. Nonpolar residues are accommodated at residues 2, 3, and 5, consistent with their location at hydrophobic regions of the binding cleft. The greatest selectivity occurs at residue 4, where significant binding was only detected with the natural substrate amino acid proline. This finding is consistent with alanine-scanning experiments (*29*) and suggests that the shape and size of the central pocket beneath the arch favor binding of proline at postion 0. Residue 6 gave significant binding only with the natural substrate amino acid lysine or with the arginine replacement. Alanine-scanning studies of IscU suggested a role for Lys^{103} in binding (*29*), and Lys9 in the crystal structure of the HscA-(SBD)-ELPPVKIHC complex was found to be involved in interactions with HscA residue Glu^{406} (*31*). The finding that only arginine can substitute for lysine at this position suggests that a salt bridge between Lys^{103} of IscU and Glu^{406} of HscA contributes to complex stabilization and substrate selectivity.

Peptide Array Binding by HscA(F426A) and HscA-(M433V). To gain insight into structural features of HscA that contribute to substrate specificity, we probed the peptide array with two HscA mutants containing "DnaK-like" substitutions near the central region of the peptide-binding cleft, F426A and M433V (see Figure 1). DnaK favors substrates enriched in leucine (*15*), and we were particularly interested in examining the ability of these mutant forms of HscA to bind peptides containing leucine substitutions. An expanded view of the leucine-substituted row of the peptide array probed with wild-type HscA, HscA(F426A), and HscA-(M433V) is shown in the right panel of Figure 2. The binding pattern for HscA(F426A) is similar to that of wild-type HscA, indicating that replacement of Phe^{426} with alanine is not sufficient to impart DnaK-like binding specificity at position 0. In contrast, replacement of Met^{433} with valine allowed for the binding of the ELPLVKI peptide. The mutant HscA-(M433V) recognizes the peptide with the leucine replacement at residue 4 (indicated by the arrow in Figure 2) in addition to the peptides recognized by wild-type HscA and HscA-(F426V). Binding of the leucine-substituted peptide by HscA-(M433V) suggests that Met^{433} is critical to the substrate selectivity of HscA and that substitution of a residue with a smaller sidechain may be sufficient to impart broader, DnaK-like substrate selectivity.

Fluorescence Measurements of HscA Binding to ELPPVKI and ELPLVKI Peptides. The peptide array binding experiments provide a qualitative picture of substrate-binding specificity but do not provide a quantitative measure of binding affinities or kinetics. We therefore employed a fluorescence-based solution peptide-binding assay (*30*) to better compare substrate affinities of the HscA(F426A) and HscA(M433V) mutants relative to wild-type HscA. This approach involves the incorporation of the F426A and M433V substitutions into HscA proteins containing a unique cysteine site for bimane labeling and the use of tryptophan peptides for quenching of bimane fluorescence. We previously found that neither N- or C-terminal tryptophan labels nor the attachment of a bimane probe via Cys^{455} significantly alters HscA-peptide interactions, indicating that this assay is capable of providing a measure of peptide affinity (*30*). For the binding of IscU-derived peptides, we used HscA mutants containing a bimane-labeling site at Cys^{455} on the backside of the SBD (cf. Figure 1 of ref *27*) and derivatives of the ELPPVKI peptide containing an N-terminal tryptophan (W-PP and W-PL; see Table 1 for peptide designations). Preliminary experiments demonstrated that the F426A and M433V substitutions did not affect the directional binding preference of HscA for these peptides (data not shown).

To assess the binding of W-PP and W-PL peptides, we recorded emission spectra of bimane-labeled HscA(A455C), HscA(F426A/A455C), and HscA(M433V/A455C) prior to and following successive peptide additions (Figure S1 in the Supporting Information). Fluorescence of the bimane-labeled HscA derivatives was quenched by W-PP and W-PL in a concentration-dependent manner. Integrated emission spectra were used to calculate the fractional fluorescence quenching following each peptide addition, and the data were fit to hyperbolic saturation functions (Figure 3). As expected, HscA(A455C)-bimane exhibits a higher affinity for the "natural" W-PP peptide ($K_d = 17\ \mu M$) than for the leucine-substituted W-PL peptide ($K_d = 77\ \mu M$). Bimane-labeled HscA(F426A/A455C) exhibited a general decrease in binding affinity relative to wild-type HscA but retained a preference for the W-PP peptide ($K_d = 100\ \mu M$) relative to the W-PL peptide ($K_d = 205\ \mu M$). In contrast, the M433V substitution reversed the binding preference for the two peptides. HscA-(M433V/A455C) favored binding of the W-PL peptide ($K_d = 56\ \mu M$) relative to the W-PP peptide ($K_d = 86\ \mu M$). These results support the conclusion from the peptide array studies that residue 433 near the base of the central peptide-binding pocket plays a key role in substrate discrimination by HscA.

The small difference in the equilibrium binding affinities of HscA(M433V) ($K_d = 56\ \mu M$) and wild-type HscA ($K_d = 77\ \mu M$) for the W-PL peptide is somewhat surprising in view of the binding difference observed in the peptide array blot in Figure 2. We therefore carried out kinetic experiments to determine whether the difference observed in the array blot reflected differences in the rates of dissociation of peptide substrates from the two proteins. As shown in Figure 4, bimane-labeled HscA(A455C) exhibits a dissociation rate ($k_{off} = 0.13\ s^{-1}$) for the W-PL peptide that is ~6-fold faster than for the W-PP peptide ($k_{off} = 0.023\ s^{-1}$). This difference in dissociation rates is consistent with the finding in the array

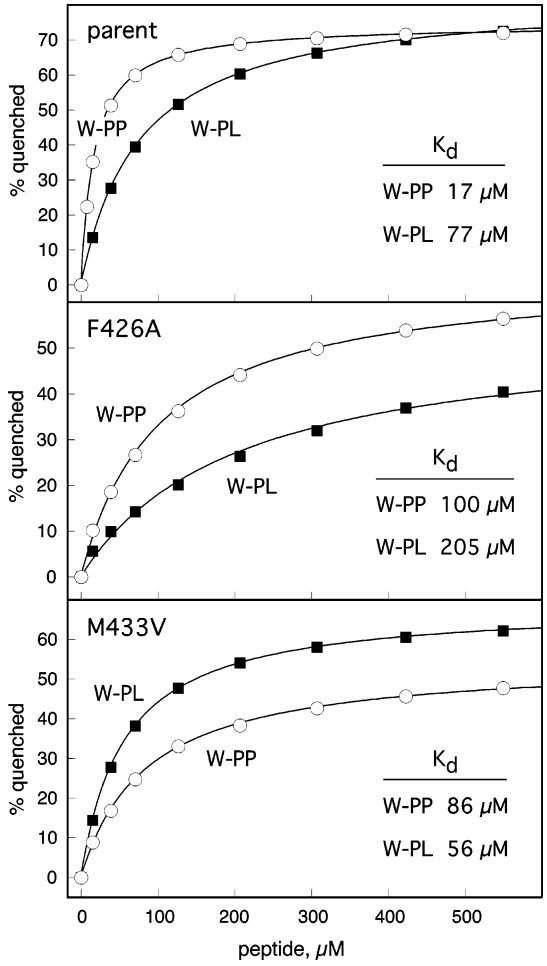

FIGURE 3: Binding of WELPPVKI (W-PP) and WELPLVKI (W-PL) peptides to bimane-labeled HscA. Fractional quenching values determined from the integrated emission intensities (see Figure S1 in the Supporting Information) are plotted versus the peptide concentration and fit to hyperbolic saturation functions. Values used to generate curves: HscA(A455C)-bimane, W-PP (○) (K_d = 17 μM, max quenching = 74%), W-PL (■) (K_d = 77 μM, max quenching = 83%); HscA(F426A/A455C)-bimane, W-PP (○) (K_d = 100 μM, max quenching = 67%), W-PL (■) (K_d = 205 μM, max quenching = 55%); HscA(M433V/A455C)-bimane, W-PP (○) (K_d = 86 μM, max quenching = 55%), W-PL (■) (K_d = 56 μM, max quenching = 70%).

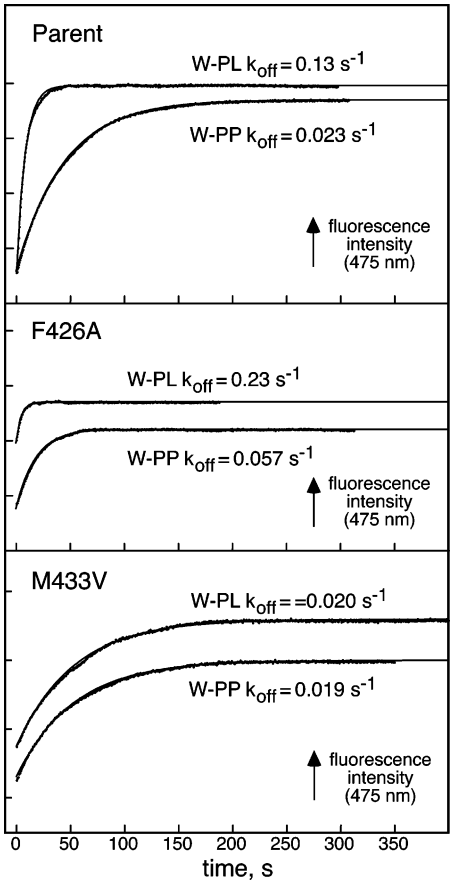

FIGURE 4: Dissociation kinetics of HscA−peptide complexes. Pre-equilibrated solutions of 100 μM bimane-labeled HscA(A455C), HscA(F426A/A455C), or HscA(M433V/A455C) and W-PP or W-PL peptide (535 μM) were diluted 80-fold with HKM buffer, and the resulting increase in fluorescence was monitored. Data were fit to a single-exponential equation to obtain peptide dissociation rates (k_{off}).

blot that wild-type HscA was not detected binding the Pro4→Leu substituted peptide. In equilibrium binding experiments, the F426A substitution resulted in a general reduction in binding affinity (Figure 3), and in the kinetic studies, dissociation rates for both the W-PP (k_{off} = 0.057 s^{-1}) and W-PL (k_{off} = 0.23 s^{-1}) peptides were 2−3-fold faster than wild-type HscA, contributing to the reduced affinity (Figure 4). As with wild-type HscA, however, the rate of peptide dissociation from HscA(F426A/A455C) is faster (∼4×) for the W-PL peptide, consistent with the lack of binding to the Pro4→Leu substituted peptide in the array blot. HscA(M433V/A455C), on the other hand, exhibited dissociation rates for both the W-PP (k_{off} = 0.019 s^{-1}) and W-PL (k_{off} = 0.020 s^{-1}) peptides similar to that for wild-type HscA and the W-PP peptide (k_{off} = 0.023 s^{-1}). The slow rate of dissociation of the W-PL peptide from HscA(M433V/A455C) in solution is consistent with the observed binding of HscA(M433V) to the Pro4→Leu substituted peptide in the array blot experiment. These findings further demonstrate that protein binding to peptide arrays is sensitive to peptide dissociation rates and underscore the need for caution when interpreting qualitative results obtained using this approach.

HscA Binding to the Model DnaK Substrate NRLLLTG. The peptide NRLLLTG (NR) has been used extensively as a model DnaK substrate (*8*, *11*, *12*, *14*, *27*, *28*, *36*−*38*), but because of the central leucine residues, this peptide is not expected to interact favorably with HscA. Because replacement of HscA Met^{433} with valine resulted in a more DnaK-like substrate specificity, we examined the binding of NR peptide derivatives to bimane-labeled forms of wild-type HscA, HscA(F426A), and HscA(M433V). The orientation in which the NRLLLTG peptide would bind was not known, and we therefore carried out initial fluorescence quenching experiments using both N- and C-terminal tryptophan-labeled peptides (W-NR and NR-W, respectively; see Table 1). Titrations were carried out by monitoring the quenching of bimane emission spectra as described for the ELPPVK-derived peptides (Figure S2 in the Supporting Information), and the results are presented as fractional quenching as a function of the peptide concentration in Figure 5. For all three forms of HscA, the highest degree of quenching was achieved by the addition of the NR-W peptide (■), consistent with the positioning of the C terminus of the bound peptide in close proximity to residue 455 on the backside of the HscA

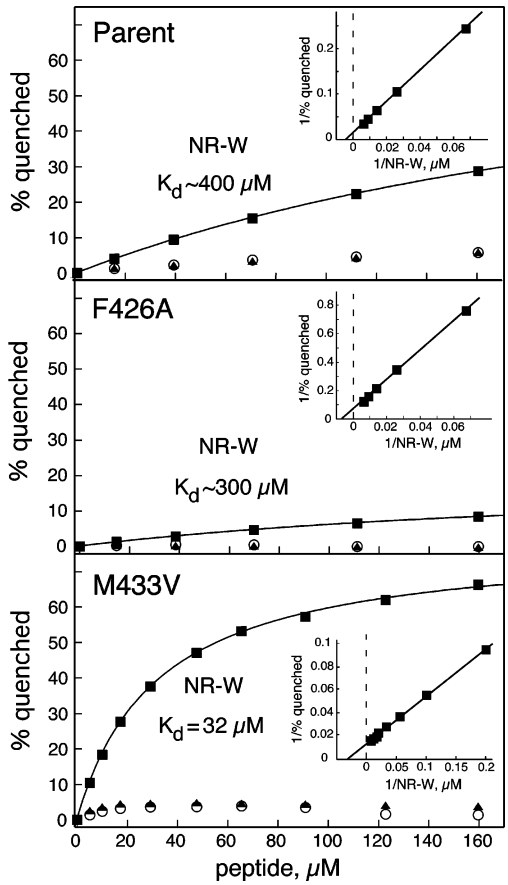

FIGURE 5: Binding of NRLLLTG peptides to bimane-labeled HscA(A455C), HscA(F426/A455C), and HscA(M433V/A455C). Emission spectra were collected prior to and following successive additions of W-NR, NR-W, or NR (see Figure S2 in the Supporting Information), and the percent of fluorescence intensity quenched was plotted versus the peptide concentration. Data for the NR-W peptide (■) were fit to hyperbolic saturation functions. Values used to generate curves: HscA(A455C)-bimane, K_d = 400 μM, max quenching = 80%; HscA(F426A/A455C)-bimane, K_d = 300 μM, max quenching = 22%; HscA(M433V/A455C)-bimane, K_d = 32 μM, max quenching = 80%. The insets show double-reciprocal plots for the NR-W peptide titrations. Data for the W-NR (○) and NR (▲) peptides were not fit.

SBD. This indicates that the NR peptides bind to HscA in the *forward* direction. This binding orientation is opposite that observed for the HscA-ELPPVKI peptide complexes (Figure 3; *30*, *31*) but is the same as observed for the NR peptide binding in the DnaK(SBD)-NRLLLTG crystal structure (*27*) and full-length DnaK in solution (*39*). The finding that the preferred orientation for peptides binding to HscA is sequence-dependent agrees with our previous studies on DnaK (*39*). In that work, peptides containing proline in the central positions were found to bind in the opposite direction of peptides containing leucine residues, and modeling studies suggested that geometrical constraints of proline residues restrict the peptide conformation to one that favors the reverse-binding orientation (*39*).

The affinity of the NR-W peptide for the HscA(A455C)- and HscA(F426/A455C)-bimane derivatives (~400 and ~300 μM, respectively) is weaker than that observed for the IscU-derived peptide W-PP (K_d = 17 and 100 μM, respectively; Figure 3), consistent with the preference of HscA for peptides containing proline in the central position. In contrast, the affinity of the HscA(M433V/A455C)-bimane derivative for the NR-W peptide is higher than that observed for either the W-PP and W-PL peptides (K_d = 85 and 56 μM, respectively; Figure 3). In addition, the M433V mutant bound the NR-W peptide with an affinity only 2-fold lower than that of the "natural" W-PP peptide for "wild-type" HscA(A455C) (K_d = 32 versus 17 μM). These binding affinities may be influenced to some degree by interactions between the bimane and tryptophan labels, but the relative affinities observed are consitent with a more DnaK-like substrate specificity for the HscA(M433V) mutant, i.e., a preference for peptides enriched in leucine and lacking proline residues. Wild-type HscA, on the other hand, favors substrates enriched in proline and disfavors leucine residues in the central position (compare Figures 2 and 3).

DISCUSSION

Functional specialization during amplification and diversification of Hsp70 chaperones has resulted in considerable divergence of substrate specificity among different family members (*7*). The high degree of conservation of the general features of the substrate-binding region, however, has made it difficult to identify key determinants of substrate selectivity. Bukau and co-workers noted that residues forming the central hydrophobic cavity of the substrate cleft exhibit a limited number of conservative substitutions, whereas residues forming the arch above the cleft are more variable (*15*). In DnaK, the arch is formed by conserved Met^{404} and Ala^{429}, and replacement of Ala^{429} with tryptophan was found to alter the affinity of DnaK for a subset of peptides (*16*). The homologous arch residues of HscA, Met^{401} and Phe^{426}, are conserved among bacterial HscA proteins, and we considered that the different substrate recognition pattern compared to DnaK might result from substitution of Phe^{426} for Ala^{429} in the arch. Peptide array and solution-binding assays carried out with HscA(F426A), however, revealed a similar substrate-binding preference to that observed for wild-type HscA. HscA(F426A) failed to show binding of the ELPL̲VKI-substituted peptide in the array blot and favored binding of PP over PL̲ peptide derivatives in the solution-binding studies. Furthermore, similar to the wild-type protein, HscA(F426A) exhibited very low affinity for the DnaK model substrate NR peptides. These findings indicate that arch residue Phe^{426} is not a major contributor to peptide-binding specificity in HscA and are consistent with the crystal structure of the HscA(SBD)-ELPPVKIHC complex, which showed that contacts with the bound peptide do not extend beyond the β carbon of Phe^{426} (*31*).

In addition to the difference in arch structure, HscA and DnaK also differ in the structure of the hydrophobic binding cleft. Met^{433} of HscA is ≅30 Å^3 larger than Val^{436} of DnaK, and this affects the size and shape of the cleft near position 0. Our previous mutagenesis studies of HscA (*29*) and the site saturation substitution array binding study presented in Figure 2 reveal that selectivity is greatest at this position and suggest that residue substitutions in this region would be most likely to affect binding specificity. Indeed, replacement of Met^{433} of HscA with valine led to significant changes in peptide-binding specificity. Unlike the wild-type protein or the arch mutant HscA(F426V), the central pocket mutant HscA(M433V) bound to a peptide having leucine in place of the central proline in the peptide array binding experiment and favored binding of leucine-substituted peptides in the

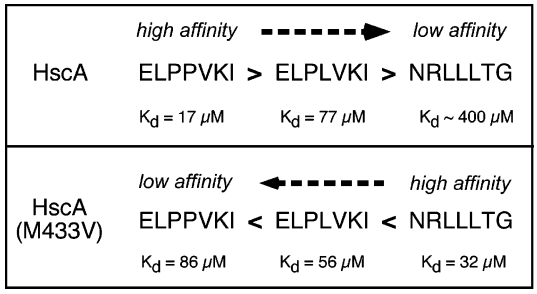

FIGURE 6: Comparison of the peptide-binding affinities of wild-type HscA and HscA(M433V).

solution-binding assays. Furthermore, solution-binding studies showed that HscA(M433V) bound the DnaK model substrate NR peptide and favored binding of this leucine-enriched peptide to the proline containing peptides PP and PL. A summary comparison of the relative binding affinities of wild-type HscA and HscA(M433V) for different peptide substrates is presented in Figure 6. Replacement of Met^{433} with valine reverses the preference of HscA from favoring peptides containing proline in central positions to those containing leucine. The reversal of the binding preference is also accompanied by a decrease in substrate selectivity: wild-type HscA exhibits about a 20-fold difference in affinity between the PP and NR peptides, whereas HscA(M433V) exhibits only about a 2.5-fold difference. Thus, while the binding pocket of HscA(M433V) is able to accommodate larger residues in the central position, the increase in size of the pocket results in a reduced ability to discriminate among peptides. A highly selective binding site is important for Hsp70 isoforms such as HscA with specific cellular roles, while the ability to interact with a wide range of substrates may be essential for chaperones with broader functions such as DnaK. It is also interesting that the NR peptide binds to HscA(M433V) in an orientation opposite that of the PP and PL peptides. This is another example of the dependence of substrate-binding orientation on peptide sequence as first described for DnaK (*39*). Changes in the binding cleft that accommodate different peptide sequences by allowing binding to occur in different directions may contribute to the broad substrate repertoire of Hsp70s having general chaperone activities.

The effect of replacement of HscA Met^{433} with valine on peptide interactions can be visualized by examining the substrate-binding domain structure near the central pocket at position 0. Figure 7 shows comparisons of structural models of different HscA and DnaK peptide complexes. The structures of the HscA-ELPPVKI (*31*; PDB ID 1U00) and DnaK-NRLLLTG (*27*; PDB ID 1DKZ) complexes are taken from the crystal structures of the substrate-binding domain−peptide complexes, and the HscA-NRLLLTG complexes were modeled by superpositioning of the HscA(SBD)-ELPPVKIHC and DnaK(SBD)-NRLLLTG structures. The HscA(M433V) structure was generated by replacing the Met^{433} sidechain in the HscA-NRLLLTG model with that of valine. The HscA-ELPPVKI complex reveals the close packing of the sidechain of Met^{433} with the central peptide residue Pro4. When the NR peptide is modeled into wild-type HscA, the sidechain of Met^{433} makes unfavorable contacts with the sidechain of the central leucine of the peptide. Steric interference between the Met^{433} and Leu^{4} would disfavor binding of the NR peptide to HscA, and this is reflected in the poor affinity of wild-type HscA for the NR peptide. Replacement of Met^{433} with valine enlarges the central hydrophobic pocket so that a leucine sidechain can be accommodated in a manner similar to that observed in DnaK. The steric clash that occurred in wild-type HscA is alleviated in HscA(M433V) allowing for favorable nonpolar interactions between the valine and leucine sidechains and resulting in higher binding affinity.

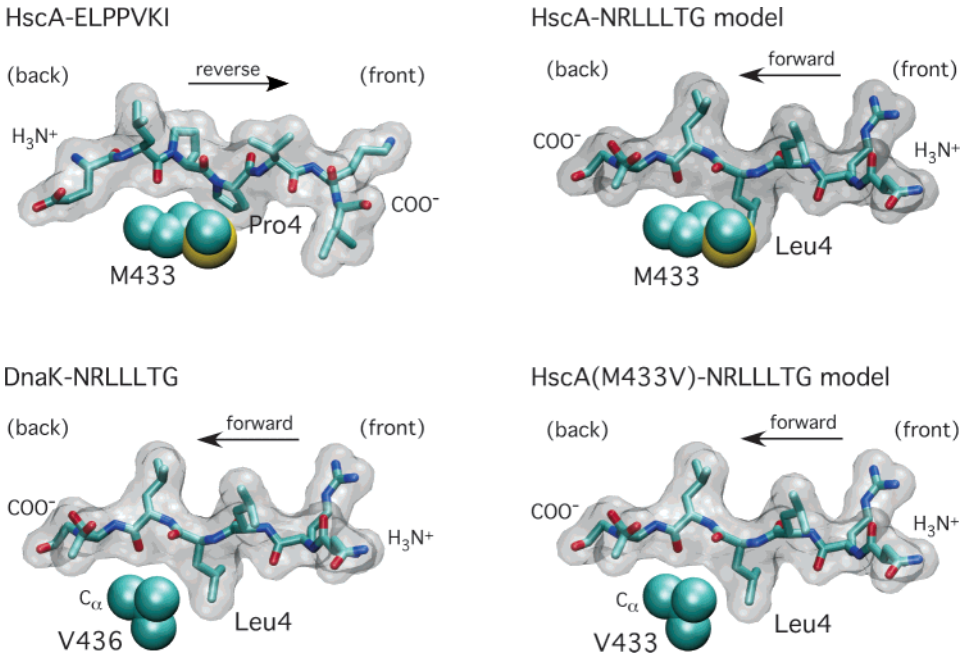

FIGURE 7: Structural representations of Hsp70−peptide interactions. HscA-ELPPVKI and DnaK-NRLLLTG complexes are adapted from refs *27* and *31*, respectively. HscA-NRLLLTG and HscA(M433V)-NRLLLTG models were generated as described in the Materials and Methods. HscA Met^{433} and DnaK Val^{436} are shown as space-filling models, and peptides are represented with gray transparent surfaces (atom color coding: carbon, cyan; nitrogen, blue; oxygen, red; sulfur, yellow). The direction of peptide binding is indicated by arrows; the front side of the substrate-binding domain is that shown in the standard view in Figure 1.

These results establish that Met^{433} makes important contributions to the substrate specificity of HscA and suggest that the homologous residue in other Hsp70s may also be critical for specificity. Additional factors, however, are also likely to contribute to substrate selection. IscU mutants with substitutions in the LPPVK recognition motif bind to HscA weakly but display normal binding affinities in the presence of the co-chaperone HscB (*29*). This underscores the importance of co-chaperone function in substrate selection (*7*, *18*−*23*). Additional residues near the binding cleft are also likely to play a role in substrate specificity. In yeast, the functional equivalent of HscA, Ssq1, recognizes a conserved LPPVK motif in the FeS-scaffold protein Isu (*40*), but the Ssq1 central binding pocket has Val^{472} at the position equivalent to HscA Met^{433}. The ability of Ssq1 to recognize the same sequence as HscA despite this difference could result from contributions of other residues in the binding region, from the targeting of Isu to Ssq1 by the co-chaperone Jac1, or a combination of the two. Studies with Isu mutants having substitutions in the Pro-Val-Lys segment revealed that Jac1 was only partially able to compensate for reduced binding (*40*), suggesting that the intrinsic specificity of the Ssq1 chaperone is important for substrate selection. Similarly, Jac1 could only partially compensate for the low Isu affinity of the mutant Ssq1(V472F) (*41*), also emphasizing the role played by the chaperone in substrate binding. Additional studies of mutant Hsp70s and their interactions with different peptide substrates should lead to a better understanding of factors determining substrate selection.

ACKNOWLEDGMENT

We thank Dennis Ta for expert technical assistance.

SUPPORTING INFORMATION AVAILABLE

Effects of W-PP and W-PL peptides (Figure S1) and NR peptides (Figure S2) on the fluorescence of bimane-labeled HscA. This material is available free of charge via the Internet at http://pubs.acs.org.

REFERENCES

1. Esser, C., Alberti, S., and Hohfeld, J. (2004) Cooperation of molecular chaperones with the ubiquitin/proteasome system, *Biochim. Biophys. Acta 1695*, 171−188.
2. Garrido, C., Schmitt, E., Cande, C., Vahsen, N., Parcellier, A., and Kroemer, G. (2003) HSP27 and HSP70: Potentially oncogenic apoptosis inhibitors, *Cell Cycle 2*, 579−584.
3. Gullo, C. A., and Teoh, G. (2004) Heat shock proteins: To present or not, that is the question, *Immunol. Lett. 94*, 1−10.
4. Asea, A. (2003) Chaperokine-induced signal transduction pathways, *Exerc. Immunol. Rev. 9*, 25−33.
5. Erbse, A., Mayer, M. P., and Bukau, B. (2004) Mechanism of substrate recognition by Hsp70 chaperones, *Biochem. Soc. Trans. 32*, 617−621.
6. Mayer, M. P., and Bukau, B. (2005) Hsp70 chaperones: Cellular functions and molecular mechanism, *Cell Mol. Life Sci. 62*, 670−684.
7. Mayer, M. P., and Bukau, B. (1998) Hsp70 chaperone systems: Diversity of cellular functions and mechanism of action, *Biol. Chem. 379*, 261−268.
8. Schmid, D., Baici, A., Gehring, H., and Christen, P. (1994) Kinetics of molecular chaperone action, *Science 263*, 971−973.
9. McCarty, J. S., Buchberger, A., Reinstein, J., and Bukau, B. (1995) The role of ATP in the functional cycle of the DnaK chaperone system, *J. Mol. Biol. 249*, 126−137.
10. Pierpaoli, E. V., Sandmeier, E., Baici, A., Schonfeld, H. J., Gisler, S., and Christen, P. (1997) The power stroke of the DnaK/DnaJ/GrpE molecular chaperone system, *J. Mol. Biol. 269*, 757−768.
11. Pierpaoli, E. V., Gisler, S. M., and Christen, P. (1998) Sequence-specific rates of interaction of target peptides with the molecular chaperones DnaK and DnaJ, *Biochemistry 37*, 16741−16748.
12. Gisler, S. M., Pierpaoli, E. V., and Christen, P. (1998) Catapult mechanism renders the chaperone action of Hsp70 unidirectional, *J. Mol. Biol. 279*, 833−840.
13. Richarme, G., and Kohiyama, M. (1993) Specificity of the *Escherichia coli* chaperone DnaK (70-kDa heat shock protein) for hydrophobic amino acids, *J. Biol. Chem. 268*, 24074−24077.
14. Gragerov, A., Zeng, L., Zhao, X., Burkholder, W., and Gottesman, M. E. (1994) Specificity of DnaK-peptide binding, *J. Mol. Biol. 235*, 848−854.
15. Rudiger, S., Germeroth, L., Schneider-Mergener, J., and Bukau, B. (1997) Substrate specificity of the DnaK chaperone determined by screening cellulose-bound peptide libraries, *EMBO J. 16*, 1501−1507.
16. Rudiger, S., Mayer, M. P., Schneider-Mergener, J., and Bukau, B. (2000) Modulation of substrate specificity of the DnaK chaperone by alteration of a hydrophobic arch, *J. Mol. Biol. 304*, 245−251.
17. Hoff, K. G., Ta, D. T., Tapley, T. L., Silberg, J. J., and Vickery, L. E. (2002) Hsc66 substrate specificity is directed toward a discrete region of the iron−sulfur cluster template protein IscU, *J. Biol. Chem. 277*, 27353−27359.
18. Pierpaoli, E. V., Sandmeier, E., Schonfeld, H. J., and Christen, P. (1998) Control of the DnaK chaperone cycle by substoichiometric concentrations of the co-chaperones DnaJ and GrpE, *J. Biol. Chem. 273*, 6643−6649.
19. Misselwitz, B., Staeck, O., and Rapoport, T. A. (1998) J proteins catalytically activate Hsp70 molecules to trap a wide range of peptide sequences, *Mol. Cell 2*, 593−603.
20. Russell, R., Wali Karzai, A., Mehl, A. F., and McMacken, R. (1999) DnaJ dramatically stimulates ATP hydrolysis by DnaK: Insight into targeting of Hsp70 proteins to polypeptide substrates, *Biochemistry 38*, 4165−4176.
21. Han, W., and Christen, P. (2003) Mechanism of the targeting action of DnaJ in the DnaK molecular chaperone system, *J. Biol. Chem. 278*, 19038−19043.
22. Silberg, J. J., Tapley, T. L., Hoff, K. G., and Vickery, L. E. (2004) Regulation of the HscA ATPase reaction cycle by the co-chaperone HscB and the iron−sulfur cluster assembly protein IscU, *J. Biol. Chem. 279*, 53924−53931.
23. Han, W., and Christen, P. (2004) cis-Effect of DnaJ on DnaK in ternary complexes with chimeric DnaK/DnaJ-binding peptides, *FEBS Lett. 563*, 146−150.
24. Hoff, K. G., Silberg, J. J., and Vickery, L. E. (2000) Interaction of the iron−sulfur cluster assembly protein IscU with the Hsc66/Hsc20 molecular chaperone system of *Escherichia coli*, *Proc. Natl. Acad. Sci. U.S.A. 97*, 7790−7795.
25. Silberg, J. J., Hoff, K. G., Tapley, T. L., and Vickery, L. E. (2001) The Fe/S assembly protein IscU behaves as a substrate for the molecular chaperone Hsc66 from *Escherichia coli*, *J. Biol. Chem. 276*, 1696−1700.
26. Kluck, C. J., Patzelt, H., Genevaux, P., Brehmer, D., Rist, W., Schneider-Mergener, J., Bukau, B., and Mayer, M. P. (2002) Structure−function analysis of HscC, the *Escherichia coli* member of a novel subfamily of specialized Hsp70 chaperones, *J. Biol. Chem. 277*, 41060−41069.
27. Zhu, X., Zhao, X., Burkholder, W. F., Gragerov, A., Ogata, C. M., Gottesman, M. E., and Hendrickson, W. A. (1996) Structural analysis of substrate binding by the molecular chaperone DnaK, *Science 272*, 1606−1614.
28. Stevens, S. Y., Cai, S., Pellecchia, M., and Zuiderweg, E. R. (2003) The solution structure of the bacterial HSP70 chaperone protein domain DnaK(393−507) in complex with the peptide NRLLLTG, *Protein Sci. 12*, 2588−2596.
29. Hoff, K. G., Cupp-Vickery, J. R., and Vickery, L. E. (2003) Contributions of the LPPVK motif of the iron−sulfur template protein IscU to interactions with the Hsc66-Hsc20 chaperone system, *J. Biol. Chem. 278*, 37582−37589.
30. Tapley, T. L., and Vickery, L. E. (2004) Preferential substrate binding orientation by the molecular chaperone HscA, *J. Biol. Chem. 279*, 28435−28442.

31. Cupp-Vickery, J. R., Peterson, J. C., Ta, D. T., and Vickery, L. E. (2004) Crystal structure of the molecular chaperone HscA substrate binding domain complexed with the IscU recognition peptide ELPPVKIHC, *J. Mol. Biol. 342*, 1265−1278.
32. Vickery, L. E., Silberg, J. J., and Ta, D. T. (1997) Hsc66 and Hsc20, a new heat shock cognate molecular chaperone system from *Escherichia coli*, *Protein Sci. 6*, 1047−1056.
33. Silberg, J. J., Hoff, K. G., and Vickery, L. E. (1998) The Hsc66-Hsc20 chaperone system in *Escherichia coli*: Chaperone activity and interactions with the DnaK-DnaJ-grpE system, *J. Bacteriol. 180*, 6617−6624.
34. Jones, T. A. (1985) Diffraction methods for biological macromolecules. Interactive computer graphics: FRODO, *Methods Enzymol. 115*, 157−171.
35. Humphrey, W., Dalke, A., and Schulten, K. (1996) VMD−Visual molecular dynamics, *J. Mol. Graphics 14*, 33−38.
36. Cai, S., Stevens, S. Y., Budor, A. P., and Zuiderweg, E. R. (2003) Solvent interaction of a Hsp70 chaperone substrate-binding domain investigated with water-NOE NMR experiments, *Biochemistry 42*, 11100−11108.
37. Popp, S., Packschies, L., Radzwill, N., Vogel, K. P., Steinhoff, H. J., and Reinstein, J. (2005) Structural dynamics of the DnaK−peptide complex, *J. Mol. Biol. 347*, 1039−1052.
38. Zhang, J., and Walker, G. C. (1998) Interactions of peptides with DnaK and C-terminal DnaK fragments studied using fluorescent and radioactive peptides, *Arch. Biochem. Biophys. 356*, 177−186.
39. Tapley, T. L., Cupp-Vickery, J. R., and Vickery, L. E. (2005) Sequence-dependent peptide binding orientation by the molecular chaperone DnaK, *Biochemistry 44*, 12307−12315.
40. Dutkiewicz, R., Schilke, B., Cheng, S., Knieszner, H., Craig, E. A., and Marszalek, J. (2004) Sequence-specific interaction between mitochondrial Fe−S scaffold protein Isu and Hsp70 Ssq1 is essential for their in vivo function, *J. Biol. Chem. 279*, 29167−29174.
41. Knieszner, H., Schilke, B., Dutkiewicz, R., D'Silva, P., Cheng, S., Ohlson, M., Craig, E. A., and Marszalek, J. (2005) Compensation for a defective interaction of the Hsp70 Ssq1 with the mitochondrial Fe−S cluster scaffold Isu, *J. Biol. Chem. 280*, 28966−28972.

BI0606187